ESD-TR-77-171

Semiannual Technical Summary

Electrooptical Devices

31 March 1977

Prepared for the Department of the Air Force
under Electronic Systems Division Contract F19628-76-C-0002 by

Lincoln Laboratory

MASSACHUSETTS INSTITUTE OF TECHNOLOGY

LEXINGTON, MASSACHUSETTS

The work reported in this document was performed at Lincoln Laboratory, a center for research operated by Massachusetts Institute of Technology, with the support of the Department of the Air Force under Contract F19628-76-C-0002.

The views and conclusions contained in this document are those of the contractor and should not be interpreted as necessarily representing the official policies, either expressed or implied, of the United States Government.

This technical report has been reviewed and is approved for publication.

FOR THE COMMANDER

Raymond L. Loiselle, Lt. Col., USAF
Chief, ESD Lincoln Laboratory Project Office

MASSACHUSETTS INSTITUTE OF TECHNOLOGY
LINCOLN LABORATORY

ELECTROOPTICAL DEVICES

SEMIANNUAL TECHNICAL SUMMARY REPORT
TO THE
ROME AIR DEVELOPMENT CENTER

1 OCTOBER 1976 – 31 MARCH 1977

ISSUED 18 AUGUST 1977

LEXINGTON MASSACHUSETTS

ABSTRACT

The current objectives of the electrooptical device program are: (1) to perform life tests on GaInAsP/InP double-heterostructure (DH) diode lasers operating in the 1.0- to 1.2-μm wavelength region and analyze the degradation mechanisms, and (2) to fabricate and study avalanche photodiodes of similar composition GaInAsP operating in the same wavelength region.

In the diode laser part of the program, 11 DH GaInAsP/InP lasers, operating continuously at room temperature, have been placed on life test. The first three devices, fabricated from one wafer, have logged over 4000, 3600, and 3200 hours, respectively, without degradation, and are still in operation. The eight devices fabricated from two additional wafers also show no evidence of internal degradation. However, a laser end-face contamination problem is present in several of the newer devices. Although this contamination can be removed from most of the devices by simple cleaning, improved fabrication procedures are currently being developed to eliminate the sources of the contamination.

The p-n junction location in DH GaInAsP/InP diode lasers has been determined by use of a scanning electron microscope. Even though undoped or Sn-doped quaternary layers are n-type if grown on insulating substrates, the quaternary layers in the lasers are p-type, presumably due to Zn diffusion from the Zn-doped InP capping layer.

As part of the avalanche photodiode program, proton bombardment and ion implantation in InP have been investigated for use in diode fabrication. A study of proton bombardment in InP indicates that the resistivity of n-type InP can be increased only to a level of about 10^3 Ω-cm, while the resistivity of p-type InP can be increased to $>10^8$ Ω-cm for an optimum multiple-energy dose or an optimum combination of dose and post-bombardment anneal. The results can be explained by a model which assumes that the proton bombardment creates both deep donor and deep acceptor levels.

The ion implantation of Se, Si, Be, Mg, Cd, and Fe in InP is under investigation. As expected, Se and Si implants followed by a 750°C, 15-min. anneal result in n-type layers, while Be, Mg, and Cd implants followed by a similar anneal result in p-type layers. Implantation of Fe has been found to be quite effective in creating high-resistivity layers in n-type InP. A multi-energy Fe implant in n-type InP ($n \approx 4 \times 10^{16}$ cm^{-3}) followed by annealing at 725°C for 15 min. yields layers with a resistivity of approximately 10^7 Ω-cm.

In the liquid-phase epitaxy (LPE) of InP for avalanche photodiodes, a high distribution coefficient impurity, identified as silicon, has been shown to be a key problem in achieving required high-purity layers. It was found not only that the Si concentration of as-received In is too high, but also that the LPE growth solution can be contaminated with Si through direct or indirect contact with quartz if a strongly reducing gas such as dry H_2 is present in the growth tube.

CONTENTS

I. 4000-HOUR CONTINUOUS CW OPERATION OF DOUBLE-HETEROSTRUCTURE GaInAsP/InP LASERS

State-of-the-art fused silica fibers have both minimum attenuation[1] and minimum dispersion[2] in the 1.1- to 1.3-μm region. Diode lasers with emission wavelengths in this region would therefore be optimum light sources for fiber optics communication systems if they had long enough operating times. Three ternary and quaternary double-heterostructure (DH) systems have been explored for use in this region, namely, GaAsSb/AlGaAsSb,[3-5] InGaAs/InGaP,[6] and GaInAsP/InP,[7-10] and CW operation at room temperature has been achieved for all three systems. However, operating times longer than 21 hrs have not been reported for any of these devices. In this report, we discuss our initial results on life tests of DH GaInAsP/InP lasers. The first three lasers to be put on life test have been in continuous operation at room temperature in an ambient air for 4000, 3600, and 3200 hrs, respectively, without evidence of degradation. These lasers, which emit at 1.15 μm, are still in operation. Additional devices from new wafers with emission wavelengths near 1.22 μm have recently been put on test.

The GaInAsP/InP lasers are stripe-geometry devices made by proton bombardment of heterostructures prepared by growing successive liquid-phase-epitaxial (LPE) layers of InP, GaInAsP, and InP on (111)B-oriented melt-grown InP substrates. For a typical 1.15-μm laser, the thickness, dopant, and carrier concentration of each LPE layer are listed in Table I. The stripe width is 13 μm, and the cavity length is 380 to 400 μm. The fabrication procedure is discussed in greater detail in Appendices A and B (Refs. 8 and 9).

TABLE I
LPE LAYERS OF GaInAsP/InP DOUBLE HETEROSTRUCTURE

Layer	Material	Thickness (μm)	Dopant	Carrier Concentration (cm^{-3})
1	n-InP	2	Sn	4×10^{18}
2	n-$Ga_{0.16}In_{0.84}As_{0.39}P_{0.61}$	0.5	Sn	3×10^{17}
3	p-InP	2	Zn	3×10^{18}

For room-temperature CW operation, each diode is indium soldered (grown side down) to a copper block which is inserted in the life test setup. The initial three devices are operating in a comparatively crude setup consisting of a copper heat sink, through which methanol is cycled to maintain the heat-sink temperature at 24 ± 2°C. During operation, the temperature of the active region of the laser, as determined from the measured temperature dependence of the emission wavelength, is about 10°C higher than the heat-sink temperature. A new, more sophisticated setup described later in this report is being used for more recently initiated tests. The laser output power is monitored continuously with a calibrated silicon solar cell, and the

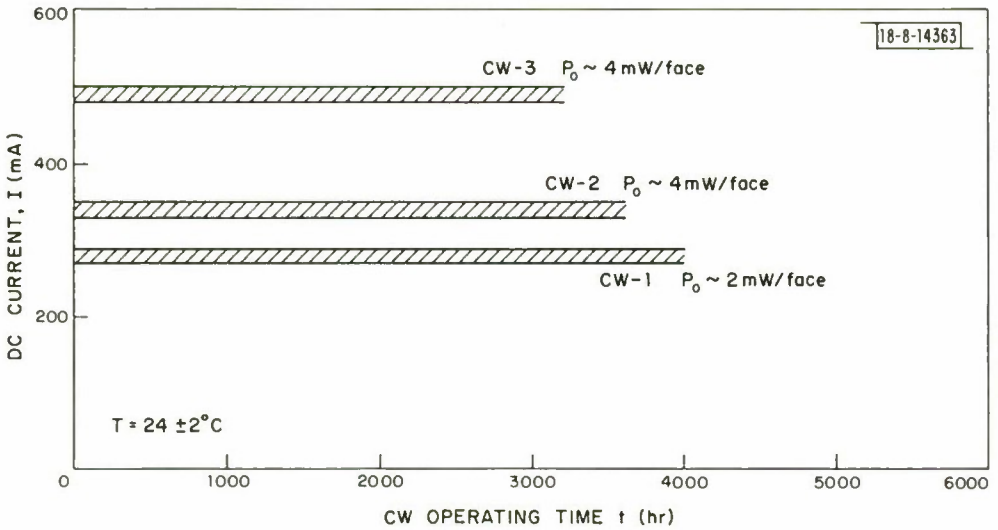

Fig. 1. Diode eurrent vs operating time for threc CW GaInAsP/InP DH lasers CW-1, CW-2, and CW-3 with single-facet output powers of 2, 4, and 4 mW (±20 percent), respectively, at an emission wavelength of ~1.15 μm.

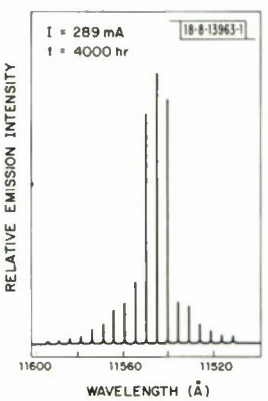

Fig. 2. Spectrum of laser CW-1, after 4000 hrs of room-temperature CW operation.

DC operating current is adjusted periodically to keep the output power constant to within ±20 percent. The threshold current is checked periodically, and the laser spectrum is measured from time to time by focusing the radiation into a grating spectrometer provided with a cooled S-1 photomultiplier.

Figure 1 shows the diode operating current as a function of time for GaInAsP/InP lasers CW-1, CW-2, and CW-3 over their first 4000, 3600, and 3200 hrs, respectively. The lasers are maintained at constant output of 2 mW for CW-1 and 4 mW for CW-2 and CW-3. No significant changes in the operating current have been observed; the small changes in current shown in Fig. 1 were due to changes in the heat-sink temperature, not to laser degradation. The threshold currents (275, 330, and 450 mA, respectively) also varied somewhat with temperature, but otherwise remained constant with time. Figure 2 shows the output spectrum of laser CW-1 at 289 mA after 4000 hrs of CW operation. The spectrum is identical to that obtained at the same current prior to the lifetime tests. Our measurements also indicate that the differential quantum efficiencies of these devices, which are typically 10 to 11 percent per face, have also remained unchanged.

Two new wafers have been successfully processed and fabricated into proton-defined stripe lasers with threshold current densities of approximately 5 kA/cm^2. Eight of these lasers, emitting at 1.22 μm with power outputs of 2 to 4 mW per face, are now on life test in a new life test setup, which is shown in Fig. 3. This new setup employs a thermoelectric heater/cooler assembly and a temperature controller to maintain the heat-sink temperature to within 0.1°C. Each individual laser, mounted in a diode package for CW operation, is attached to the heat sink and is enclosed in a chamber with provision for control of the ambient atmosphere. Operating current for each device is provided by a separate current supply which can be adjusted to within

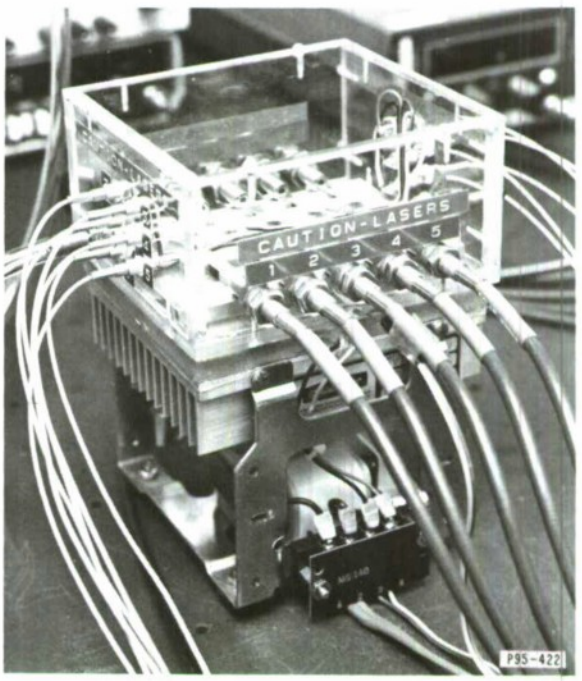

Fig. 3. Photograph of improved life-test setup.

0.1 mA. Optical fibers are utilized for output coupling, and the light output of each device is monitored by a large-area germanium photovoltaic cell.

Several devices recently tested appear to suffer from contamination of the laser end faces, resulting in a reduction of output power. The problem has been traced to inadequate cleaning procedures prior to and after packaging of the laser. One suspected source of the contamination is incomplete removal of the flux used in the mounting process. Improved cleaning techniques as well as methods for facet protection are under development and show considerable promise.

The dependence of threshold current as a function of active layer thickness has also been measured for several devices. The thickness for the active layer was determined from an SEM (scanning electron microscope) photomicrograph of the cleaved and etched facet of each device. For lasers emitting at 1.15 to 1.22 μm, the active layer thickness for minimum threshold current is in the 0.1- to 0.2-μm range. The lowest pulsed thresholds of 2.2 kA/cm^2 on a broad-area device and 5 kA/cm^2 on a stripe-geometry laser were obtained on a wafer with an active layer 0.12 μm in thickness.

These initial life-test data on GaInAsP/InP lasers provide a very encouraging indication that devices of this type will prove to be sufficiently reliable for use as light sources in fiber optics communication systems. It is of particular interest that the lasers are fabricated from heterostructures grown on InP substrates with dislocation densities of about 5×10^5 cm^{-2}, since GaAs/AlGaAs lasers grown on substrates with such high dislocation densities would have very short lifetimes.[11] This suggests that GaInAsP/InP lasers may not be subject to the same degradation mechanisms that are responsible for the failure of GaAs/AlGaAs lasers.[12]

C. C. Shen
J. J. Hsieh
T. A. Lind

II. DETERMINATION OF THE p-n JUNCTION LOCATION IN DOUBLE-HETEROSTRUCTURE GaInAsP/InP DIODE LASERS

The actual position of the p-n junction in DH GaInAsP/InP lasers has been investigated by means of a scanning electron microscope. The DH samples, which are similar to those described in the previous section, were prepared by growing successive LPE layers of n-InP, n-GaInAsP, and p-InP on (111)B-oriented melt-grown n-InP substrates. The two barrier layers, namely n-InP and p-InP, were doped with Sn and Zn, respectively, to a carrier concentration $\sim 3 \times 10^{18}$ cm^{-3} and the GaInAsP active layers were either undoped or Sn-doped. The as-grown GaInAsP layers were determined to be n-type with carrier concentrations varying from 10^{16} to 10^{17} cm^{-3}, as determined from Hall measurements made on layers grown under the same conditions on semi-insulating InP substrates. Both InP layers are 2 to 3 μm thick, while the thickness of the GaInAsP layer varied from 0.1 to 1 μm. The growth temperature and the growth time for the p-InP layer are typically 620°C and 10 min., respectively.

The wafers were processed into broad-area lasers, following the fabrication procedures described earlier (Appendix B and Ref. 9). Devices with normal I-V characteristics and mirror-like cleaved facets were selected for further investigations.

The heterojunction interfaces were delineated by etching the cleaved cross sections in a solution of $3H_2SO_4:1H_2O_2:1H_2O$ at room temperature for 20 sec. The cleaved faces were examined in the SEM, both in the usual secondary emission mode and in the induced current mode.

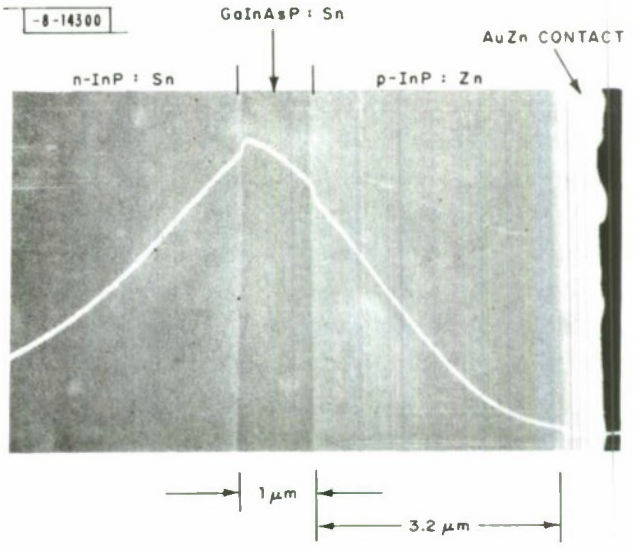

Fig. 4. SEM photomicrograph of the cleaved and etched cross section of a DH GaInAsP/InP laser. An induced current trace was superimposed on the secondary emission image (X 13,000).

In the latter, the display was deflection modulated by the p-n junction current due to electron-hole pairs generated by the scanning electron beam. A SEM photomicrograph of the cleaved section of a typical broad-area device is shown in Fig. 4. The two heterojunction interfaces between the InP and GaInAsP layers are revealed in the secondary emission image, and the location of the p-n junction is identified by the peak of the superimposed induced current trace. For all the devices tested to date, the p-n junction was found to coincide with the n-InP/GaInAsP interface to within 0.1 μm, which indicates that the GaInAsP layer has been converted to p-type during the growth of the p-InP layer. This phenomenon is presumably due to the diffusion of Zn from the p-InP layer through the GaInAsP region. Note that the n-InP layer remained n-type. This is the result of the fact that the n-InP layer is so heavily doped that the amount of Zn which diffused into this layer was insufficient to convert it to p-type. As a result, the p-n junction was located at the n-InP/GaInAsP interface. For the sample shown in Fig. 4, the effective Zn diffusion coefficient in the GaInAsP region is estimated to be 1.4×10^{-11} cm^2 sec^{-1} at 620°C. This value is the same order of magnitude as that reported for InP[13] at a diffusion temperature of 650°C using a chemical diffusion method.

These results suggest that the fast diffusion of Zn in GaInAsP causes a shift of the p-n junction during the growth process. In order to prevent the p-n junction from occurring in the n-InP, a heavily doped n-InP layer (i.e., 3×10^{18} cm^{-3}) is required.

C. C. Shen
J. J. Hsieh

III. PROTON BOMBARDMENT IN InP

Proton bombardment has previously been used to make high-resistivity layers in both p- and n-type GaAs,[14-17] $Al_xGa_{1-x}As$,[17,18] and GaP,[19] and this technique has been applied to the fabrication of a number of different microwave and optoelectronic devices (for a summary of applications see Ref. 20). Recently, proton bombardment was used successfully to fabricate

stripe-geometry GaInAsP/InP lasers.[9] Although the resistivity of the bombarded p-InP region was apparently increased sufficiently to confine the diode current to the stripe, the electrical properties of the bombarded InP were not measured. In this section, we describe the initial results of a study of the effects of proton bombardment on the electrical properties of n- and p-type InP. Unlike results in the Ga-based III-V compounds, it is found that the resistivity of n-type InP can be increased only to about 10^3 Ω-cm, whereas that of p-type InP can be increased to $>10^8$ Ω-cm for an optimum proton dose. A simple model appears to explain the experimental results obtained up to this time.

The InP samples used in these experiments were cut from bulk (111)-oriented n-type, p-type and high-resistivity ($\rho \approx 10^7$ Ω-cm) crystals. The carrier concentrations of the n-type samples ranged from 1×10^{16} to 1×10^{18} cm^{-3}, and those of the p-type samples from 5×10^{17} to 5×10^{18} cm^{-3}. After polishing, the B face of each sample was etched[21] in a 1:1:5:1 mixture of $HAc:HClO_4HNO_3:HCl$. Evaporated Au contacts 20 mils in diameter and <1000 Å thick were made to the samples, either prior to bombardment or, when samples were to be annealed, after bombardment and anneal. Samples to be bombarded and annealed were first coated with 1000 Å of SiO_2, deposited pyrolytically at 320°C. For the purposes of these experiments, the effects of the SiO_2 and the thin gold contacts on the range of protons could generally be neglected. A large-area, plated gold back contact was usually used to contact the substrate.

Both single-energy 400-keV and multi-energy proton bombardments were carried out with the InP samples at room temperature. As in carlier results on n^+-GaAs,[22] a multiple-energy proton bombardment was generally found to be superior to a single-energy bombardment. The multi-energy bombardment schedule used was based on a dose of N at 400 keV, 0.6 N at 300 keV, 0.3 N at 200 keV, and 0.2 N at 100 keV, where N is the dose at 400 keV in cm^{-2}. (There is some indication that an additional dose of 0.1 N at 50 keV may provide an even more "uniform-damage" region.) The depth to which this bombardment schedule affects the resistivity of the InP was found to be approximately 3.8 μm, as determined from the capacitance (5.9 pF) of a 20-mil-dia. Au contact on p-type InP bombarded with an optimum dose (see below).

For bombarded n-type InP, thc current-voltage characteristics of the Au-InP contacts are generally linear.* The contact-to-substrate resistance increases with proton dose up to a maximum value of 550 to 800 Ω, irrespective of initial carrier concentration, although devices on samples with lower initial concentrations generally have the higher maximum resistances. These maximum resistance values correspond to an average resistivity in the bombarded region of about (3 to 4) $\times 10^3$ Ω-cm. The minimum dose required to achieve this resistivity increases slightly with increasing initial carrier concentration, with multi-energy bombardment at $N = 1 \times 10^{15}$ cm^{-2} (see above schedule) being generally sufficient for 1×10^{18} cm^{-3} material. For further increase in dose, the resistivity begins to decrease slightly.

On unbombarded or lightly bombarded p-type InP, the electrical characteristics of the Au-InP contacts are those of a Schottky barrier on p-type material. With increasing proton dose, the current-voltage characteristics become more symmetrical, the resistance increases dramatically, and the capacitance decreases to a minimum of about 5.8 pF. For a dose which maximizes the resistance, the current is linear with voltage out to at least ±25 V, with the observed resistance corresponding to a resistivity $>10^8$ Ω-cm. The optimum multiple-energy dose corresponds to a N of approximately 3×10^{13} cm^{-2} for material with $p = 5 \times 10^{17}$ cm^{-3}, and

* The gold contacts on InP samples with $n < 10^{17}$ cm^{-3} behaved as leaky Schottky barriers before bombardment, but became linear after a bombardment with $N \geqslant 10^{14}$ cm^{-2}.

about 1×10^{14} cm^{-2} for $p \approx 5 \times 10^{18}$ cm^{-3} material. For doses higher than the optimum, the bombarded layer apparently becomes n-type, the resistivity decreases and the I-V characteristics of the devices begin to look like those of p-n diodes. For high doses ($N \approx 3 \times 10^{15}$ cm^{-2}), the diffusion voltage extrapolated from the forward I-V characteristics of these diodes is 0.8 to 0.9 V and the forward series resistance is approximately 900 Ω.

To confirm this apparent n-type conductivity at high doses, Hall measurements of the van der Pauw type[23] were made on heavily bombarded layers in p-type and Fe-doped (initial $\rho \approx 10^7$ Ω-cm) material. Several of the Fe-doped samples had a thin Mg ion-implanted p-type layer[24] with a sheet concentration of 4×10^{13} cm^{-2} and a mobility of 80 cm^2/V-sec. After a standard multi-energy bombardment with N ≈ (1 or 3) × 10^{15} cm^{-2}, n-type conductivity was observed on all samples. For a 3.8-μm-deep bombarded region, parameter values of $\rho \approx 200$ to 1000 Ω-cm, $n \approx (0.4 \text{ to } 1) \times 10^{14}$ cm^{-3}, and $\mu \approx 100$ to 500 cm^2/V-sec were obtained. These resistivities are somewhat lower than the $\approx 4 \times 10^3$ Ω-cm obtained from I-V measurements on the Au-InP contacts. However, the resistivities determined from the I-V measurements could be too high due to unaccounted-for series resistance, whereas those determined from the van der Pauw measurements could be too low due to current leakage through the substrates.

A simple model which appears to explain these results is shown in Fig. 5. In this model, we assume that the proton bombardment creates one or more each of both deep donor and deep acceptor levels, as shown in Fig. 5(a). It is not material to this simple model whether the donors or acceptors are closer to the conduction band edge; however, if they are associated with the same defects or complexes, the acceptor levels for any particular center would be closer to the

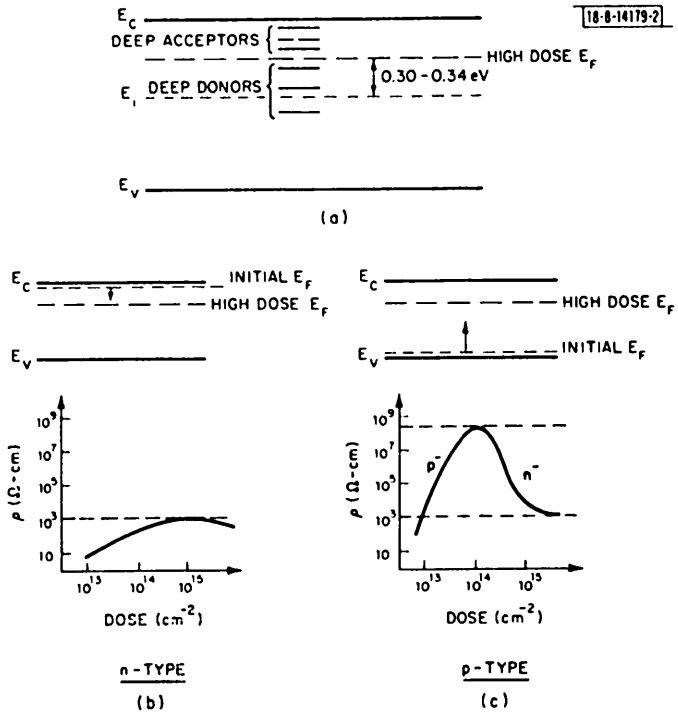

Fig. 5. Simple model for effects of proton bombardment in InP: (a) position of Fermi level for high doses, (b) effects on n-type material, and (c) effects on p-type material.

TABLE II

MULTIPLE-ENERGY PROTON BOMBARDMENT IN $p \approx 5 \times 10^{18}$ cm^{-3} InP

Sample	Proton Bombardment		No Anneal		200°C Anneal		300°C Anneal		400°C Anneal	
	Energy (keV)	Dose (cm^{-2})	R_o (MΩ)	C^* (pF)	R_o (MΩ)	C^* (pF)	R_o (MΩ)	C^* (pF)	R_o (MΩ)	C^* (pF)
1	400	1.0×10^{14}	⩾50	6.5	⩾100	6.0	Schottky barrier	83.2	–	–
	300	6.0×10^{13}								
	200	3.0×10^{13}								
	100	2.0×10^{13}								
2	400	3.0×10^{14}	$n^- - p$ Junction	11.1	≈5MΩ	5.8	⩾25	6.0	Schottky barrier	28.0
	300	1.8×10^{14}								
	200	9.0×10^{13}								
	100	6.0×10^{13}								
3	400	3.0×10^{15}	$n^- - p$ Junction	76.5	$n^- - p$ Junction	40.7	$n^- - p$ Junction	29.2	⩾30	6.0
	300	1.8×10^{15}								
	200	9.0×10^{14}								
	100	6.0×10^{14}								

* Capacitance measured at 500 kHz.

For 20-mil diameter contact on ideal 3.8-μm thick 10^8 Ω-cm layer, R_o = 18 MΩ and C = 5.8 pF.

conduction band edge. In n-type material, the Fermi level moves downward with increasing proton dose, until it becomes pinned at a position designated as the high-dose Fermi level, as shown in Fig. 5(b). Because of some spread in the measured high-dose resistivities and uncertainty in the value for the mobility, the high-dose Fermi level can be located only within a range 0.3 to 0.34 eV above the intrinsic Fermi level. At this level, the resistivity is of the order of 10^3 Ω-cm. For very high doses, banding of the defect levels will probably produce the observed reduction in resistivity. In p-type material, the Fermi level moves upward with increasing proton dose, as shown in Fig. 5(c). When the Fermi level reaches a point near the intrinsic Fermi level the resistivity becomes a maximum. For still higher doses, the Fermi level continues to move toward the conduction band until it is pinned at the high-dose level and the bombarded layer becomes weakly n-type, as observed.

The annealing characteristics of these proton-bombarded InP layers are also of interest, and the behavior was found to be qualitatively similar to that reported for proton-bombarded GaP[19] and n^+-GaAs.[22] Table II summarizes the pertinent results obtained on p-type material with an initial carrier concentration of 5×10^{18} cm^{-3}. This table lists the DC resistance, R_o, measured on a curve tracer, and the capacitance, C, measured at 500 kHz, of three samples bombarded with different doses, portions of which were annealed for 15 min. at several different temperatures up to 400°C. For an ideal 3.8-μm-thick layer of 10^8 Ω-cm material, the resistance and capacitance of a 20-mil-dia. gold contact would be 18.7 MΩ and about 5.8 pF, respectively. Several points can be noted from the data of Table II. With increasing dose, the anneal temperature at which the resistivity is maximum also increases. Underannealing results in n^-p junctions with high forward resistance (as in high-dose unannealed samples), whereas overannealing results in Schottky barriers on p^- material (as in low-dose unannealed samples). This pattern of annealing characteristics can be qualitatively explained by postulating that more than one type of compensating defect or complex is being created by the proton bombardment and that each type anneals out at a somewhat different temperature.

A typical I-V characteristic of a device on sample 1 annealed at 200°C is shown in Fig. 6. The resistance at zero voltage corresponds to a resistivity of 5×10^8 Ω-cm. Very little leakage

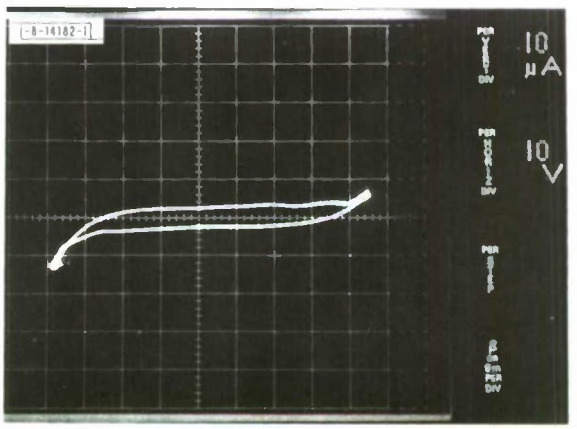

Fig. 6. Current-voltage characteristics of 20-mil-dia. gold contacts on multi-energy proton-bombarded p^+-InP ($p \simeq 5 \times 10^{18}$ cm^{-3}) sample. The InP was bombarded with proton doses of 1×10^{14} cm^{-2} at 400 keV, 6×10^{13} cm^{-2} at 300 keV, 3×10^{13} cm^{-2} at 200 keV, and 2×10^{13} cm^{-2} at 100 keV and post-annealed at 200°C for 15 min.

current flows out to ±40 V, where the average electric field is $\approx 10^5$ V/cm. The capacitance (measured at 500 kHz) of the same device, as well as devices from sample 3 annealed at 400°C, was typically 6.0 pF (slightly larger than that observed on unannealed samples[22]), and showed little variation with voltage out to ⩾45 V in either bias direction. However, the zero-bias capacitance and AC resistance measured on a bridge were found to be frequency dependent over the range 5 to 500 kHz. This is shown in Fig. 7 for devices on the same two samples. The AC

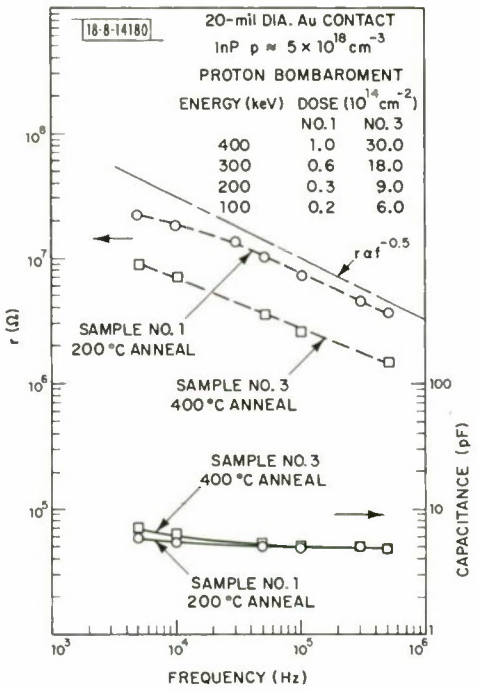

Fig. 7. The AC resistance and capacitance of 20-mil-dia. gold contacts on two multi-energy proton-bombarded p = 5 × 10^{18} cm^{-3} InP samples. The samples are Sample 1 of Table II annealed at 200°C and Sample 3 annealed at 400°C.

resistance, r, is proportional to $f^{-1/2}$ at higher frequencies, while the capacitance, C, decreases with frequency, asymptotically approaching a constant value at the higher frequencies. This type of behavior is similar to that observed in proton-bombarded n^+-GaAs,[22] and is believed to be due to a hopping type of conductivity.[25,26]

J. P. Donnelly
C. E. Hurwitz

IV. ION IMPLANTATION IN InP

Ion implantation is being investigated as a technique for fabricating avalanche photodiodes in GaInAsP. Initial studies are being carried out in InP as this material is more readily available and is quite similar in properties to GaInAsP. It is expected that the technology can be readily adapted to the quaternary material. In this section, some initial results on the use of implantation to create n-type, p-type, and high-resistivity layers in InP will be summarized. Details of the encapsulation system and of the implantation results will be given in subsequent reports.

In general, post-implantation anneal temperatures of 725° to 750°C were required to achieve high electrical activity of the implanted ion species. To protect the InP at these temperatures, a pyrolytic phosphosilicate glass (PSG) encapsulation, which permitted reproducible annealing at temperatures in excess of 750°C, was developed.

For n-type layers, 400-keV Se^+ or Si^+ ions were implanted into high-resistivity ($\rho \geq 10^7$ cm) Fe-doped InP substrates held at both room temperature and 200°C. For doses of $10^{13} Se^+/cm^2$, the sheet carrier concentration of the implanted layers did not depend on the substrate temperature, whereas the sheet mobility was consistently ≈ 20 percent higher on the samples implanted at 200°C. For doses $\geq 10^{14}$ Se^+/cm^2, higher values of both sheet carrier concentration, N_s, and mobility, μ_s, were obtained for implants made into the heated substrates. Following a 750°C, 15-min. anneal, samples implanted at 200°C with 1×10^{14} Se^+/cm^2 exhibited a N_s of 7.8×10^{13} cm^{-2} and a μ_s of 1810 cm^2/V-sec. At a dose of 1×10^{15} Se^+/cm^2, N_s and μ_s were 3×10^{14} cm^{-2} and 1300 cm^2/V-sec, respectively, which corresponds to a sheet resistivity of 16 Ω/□. The results obtained with Si^+ were similar to those using Se^+ ions.

To make p-type layers in Fe-doped InP, Be^+, Mg^+, and Cd^+ were implanted at 50, 150, and 400 keV, respectively. Mg^+ was also implanted into n-type InP ($n \approx 4 \times 10^{16}$ cm^{-3}) with results similar to those obtained in the high-resistivity substrates. Implantation of Mg^+ into substrates at room temperature resulted in higher sheet carrier concentrations than implantation into heated substrates. Samples implanted at room temperature with 1×10^{14} Mg^+/cm^2 and annealed at 750°C for 15 min. yielded values of N_s and μ_s of 5.2×10^{13} cm^{-2} and 83 cm^2/V-sec, respectively. For the heavier ion, Cd^+, however, the opposite result was found, and higher sheet carrier concentrations were obtained on samples implanted at 200°C. For a sample implanted at 200°C with 1×10^{14} Cd^+/cm^2 and annealed at 750°C, N_s and μ_s were 3.6×10^{13} cm^{-2} and 90 cm^2/V-sec, respectively.

In the preceding section it was noted that proton bombardment could convert p-type InP to high-resistivity material ($\rho \geq 10^8$ Ω-cm), but that this technique was not similarly useful for substantially increasing the resistivity of n-type material. Implantation of Fe, however, was found to be quite effective in creating high-resistivity layers in n-type InP. A multi-energy (flat profile) Fe implant in n-type InP ($n \approx 4 \times 10^{16}$ cm^{-3}) followed by a 725°C 15-min. anneal resulted in layers with a resistivity of approximately 10^7 Ω-cm.

J. P. Donnelly
C. E. Hurwitz

V. Si CONTAMINATION OF LPE InP

Our early attempts to grow high-purity InP by liquid-phase epitaxy from an In-rich solution have shown that silicon contamination is a key problem. Not only is the Si concentration in as-received In too high for our requirements, but the growth solution can be further contaminated through direct or indirect contact with quartz if a strongly reducing gas such as dry H_2 is present in the growth tube. Reports in the literature on LPE growth of high-purity InP have been incomplete in that the partial pressure of H_2O in the atmosphere of H_2 over the growth has either not been measured or has not been reported, and it is this parameter that determines the equilibrium concentration of Si in the growth solution at a given temperature. A similar situation exists for the Si contamination of Ga-rich growth solutions for GaAs growth.[27,28] However, the distribution coefficient, k_{Si}, which is the ratio of the Si concentration in the growth to that in the solution, is much less than 1 for GaAs but is ≈ 30 for InP.[29] With this large k_{Si}, the minimum donor concentration that can be expected, using our best as-received In with a few ppm Si, is $\sim 1 \times 10^{18}$ cm^{-3}.

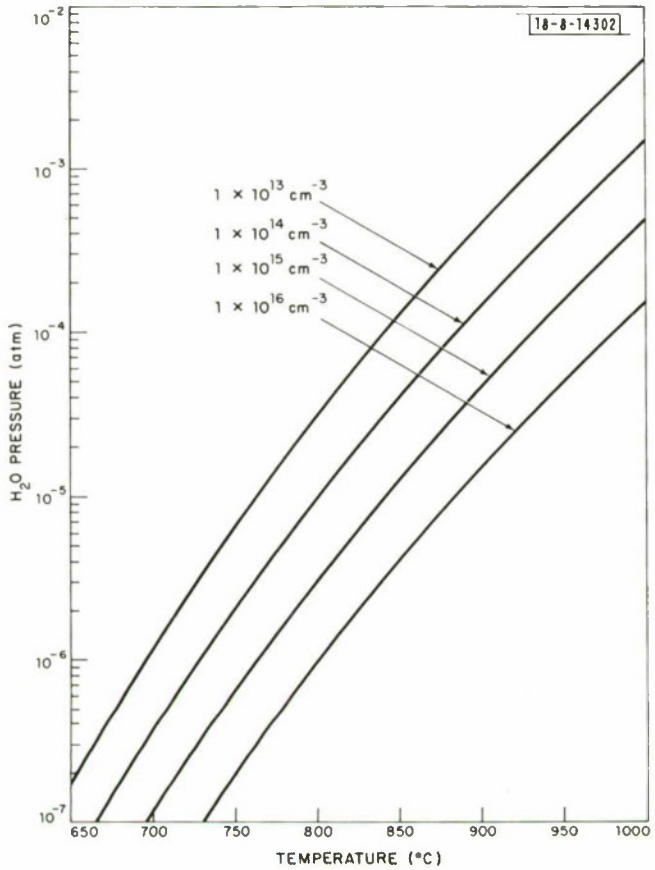

Fig. 8. Results of a calculation of the Si concentration in an In solution, in equilibrium with SiO_2, as a function of temperature and H_2O vapor pressure. Lines of constant Si concentration are labelled by the donor carrier concentration in InP grown from In-rich solution, assuming $k_{Si} = 30$.

The mechanism for Si contamination from the vapor is a two-step process. First, during baking or growth, gaseous SiO is formed by the reaction

$$SiO_2(s) + H_2(g) \rightarrow SiO(g) + H_2O(g) \quad ,$$

where s, ℓ, and g specify the solid, liquid, or gaseous phase of the substrate. In the second step, the SiO is reduced by contact with the molten In, and the Si dissolves in the solution

$$2In(\ell) + SiO(g) \rightarrow In_2O(g) + Si(\ell) \quad .$$

Weiner has worked out the kinetics of the Si contamination of a Ga solution as a function of temperature and partial pressure of H_2O (Ref. 28). By using thermodynamic values in the literature for the free energy of In_2O and the solubility of Si in In, it is possible to make similar calculations for the Si contamination of In solutions. An interesting second case considered by Weiner is that of direct Ga contact with a silica boat, whereby contamination can occur by the reaction (written here in terms of In instead of Ga)

$$SiO_2(s) + 4In(\ell) \rightarrow 2In_2O(g) + Si(\ell) \quad .$$

This reaction is of interest even without the silica boat because if driven to the left by a sufficiently high In_2O pressure (controlled by the H_2O pressure), purification of the In is achieved. The SiO_2 formed presumably floats to the surface where it either does not interfere with the growth or can be etched away. Again, it is possible to calculate the kinetics and the equilibrium values for the purification process, except that the limiting rate is expected to be set by the diffusion of Si to the In surface, rather than by the flow of gaseous reactants to the In surface, as treated by Weiner. In Fig. 8, we show results of the equilibrium concentration calculations. By assuming $k_{Si} = 30$, we have expressed the Si concentration as a minimum donor concentration in the epitaxial InP, rather than as a fraction of the growth solution. The calculations have been made using free energy values from the JANAF Tables,[30] as well as the thermodynamic data from Refs. 31 and 32.

In our experimental work, we have assembled an LPE growth system with high vacuum integrity and have reduced H_2O vapor levels in it by vacuum baking. A procedure followed in several early runs was to give the In an extended (>12 hour) bake at ~930°C under Pd-diffused H_2. Epitaxial layers grown after this treatment have very high donor concentrations up to the mid-10^{19} cm^{-3} range. Mass spectrographic analyses of the In showed that this baking treatment increased the Si content of the In from ~10 ppm to above 100 ppm. The rate of Si contamination observed is predicted by the thermodynamic calculations if the partial pressure of H_2O in our system is 10^{-8} atm, a number that is corroborated by the temperature at which the In_2O_3 on the In charge is reduced, as observed with a "transparent" furnace.

Our next efforts at In baking went to the opposite extreme by utilizing a source of H_2O-saturated H_2 mixed with the Pd-diffused H_2, giving a H_2O partial pressure of 10^{-2} atm. The Si level in the In baked in this atmosphere was not accurately determined, but it stayed under the 10-ppm level, and there were indications in the mass spectrographic analysis that the Si was concentrated at the surface, as expected if converted to SiO_2. Net carrier concentration levels in epitaxial layers grown from this In were reduced, but only to the 1×10^{17} cm^{-3} level. A bake under dry H_2 for 6 hours at 600°C reduced the net carrier concentration to the mid-10^{16} level. Our interpretation of the results with the wet H_2 baking is that the Si contamination problem has been replaced by an O_2 contamination problem. Solomon observed for growth of GaAs

from Ga-rich solution that H_2O or Ga_2O_3 added to the growth atmosphere or solution introduced donor impurities.[33] Our results are understandable if O_2 behaves in a similar way for InP grown from In-rich solution.

An apparatus for In baking is presently being assembled that will allow the ratio of H_2O to H_2 pressures to be set at any level between the very wet and very dry extremes used heretofore. With this, we will be able to compare measured donor concentrations with those prediced in Fig. 8, and we expect that this apparatus will lead to considerably higher levels of purity than we have been able to obtain to date.

S. H. Groves

REFERENCES

1. M. Horiguchi, Electron. Lett. 12, 310 (1976).
2. D. N. Payne and W. A. Gambling, Electron. Lett. 11, 176 (1975).
3. K. Sugiyama and H. Saito, Jpn. J. Appl. Phys. 11, 1057 (1972).
4. R. E. Nahory and M. A. Pollack, Appl. Phys. Lett. 27, 562 (1975).
5. R. E. Nahory, M. A. Pollack, E. D. Beebe, J. C. DeWinter, and R. W. Dixon, Appl. Phys. Lett. 26, 528 (1976).
6. C. J. Nuese and G. H. Olsen, Appl. Phys. Lett. 26, 528 (1975).
7. A. P. Bogatov, L. M. Dolginov, P. G. Eliseev, M. G. Mil'vidskii, B. N. Sverdlow, and E. G. Shevchenko, Sov. Phys.-Semicond. 9, 1282 (1975).
8. J. J. Hsieh, Appl. Phys. Lett. 28, 283 (1976).
9. J. J. Hsieh, J. A. Rossi, and J. P. Donnelly, Appl. Phys. Lett. 28, 709 (1976).
10. K. Oe and K. Sugiyama, Jpn. J. Appl. Phys. 15, 2003 (1976).
11. For a review of GaAs/AlGaAs injection lasers, see M. B. Panish, Proc. IEEE 64, 1512 (1976).
12. L Hayashi (private communication).
13. B. Tuck and A. Hooper, J. Phys. D: Appl. Phys. 8, 1806 (1975).
14. K. Wohlleben and W. Beck, Z. Naturf. 21A, 1057 (1966).
15. A. G. Foyt, W. T. Lindley, C. M. Wolfe, and J. P. Donnelly, Solid-State Electron. 12, 209 (1969).
16. J. C. Dyment, J. C. North, and L. A. D'Asaro, J. Appl. Phys. 44, 207 (1973).
17. J. C. Dyment, L. A. D'Asaro, J. C. North, B. I. Miller, and J. E. Ripper, Proc. IEEE 60, 726 (1972).
18. P. N. Favennec and D. Diquet, Appl. Phys. Lett. 23, 546 (1973).
19. S. M. Spitzer and J. C. North, J. Appl. Phys. 44, 214 (1973).
20. J. P. Donnelly, to be published in Proc. of 1976 North American Symposium on GaAs and Related Compounds, St. Louis, Missouri, 26-29 September 1976 (Inst. Phys., London).
21. R. Becker, Solid-State Electron. 16, 1241 (1973).
22. J. P. Donnelly and F. J. Leonberger, Solid-State Electron. 20, 183 (1977).
23. L. J. van der Pauw, Philips Res. Rep. 13, 1 (1958).
24. J. P. Donnelly and C. E. Hurwitz, to be presented at the 1977 Device Research Conference, Ithaca, New York, 27-29 June 1977.
25. M. Pollak and T. H. Geballe, Phys. Rev. 122, 1742 (1961).
26. A. K. Jonscher, Non-Crystalline Solids 8-10, 293 (1972).
27. H. G. B. Hicks and P. D. Greene, in Proc. 3rd Int. Symp. on Gallium Arsenide (Inst. Phys. Phys. Soc., London, Conf. Ser. No. 9, 1971), p. 92.
28. M. E. Weiner, J. Electrochem. Soc. 119, 496 (1972).
29. G. G. Baumann, K. W. Benz, and M. H. Pilkuhn, Ibid 123, 1232 (1976).
30. JANAF Thermochemical Tables (U. S. Department of Commerce, 1965).
31. P. H. Keck and J. Broder, Phys. Rev. 90, 521 (1953).
32. A. Klinedinst and D. A. Stevenson, J. Chem. Thermodynamics 5, 21 (1973).
33. R. Solomon, in Proc. 2nd Int. Symp. on Gallium Arsenide (Inst. Phys. Phys. Soc., London, Conf. Ser. No. 7, 1969), p. 11.

Room-temperature operation of GaInAsP/InP double-heterostructure diode lasers emitting at 1.1 μm*

J. J. Hsieh

Lincoln Laboratory, Massachusetts Institute of Technology, Lexington, Massachusetts 02173
(Received 27 October 1975; in final form 22 December 1975)

Double-heterostructure $Ga_{0.12}In_{0.88}As_{0.23}P_{0.77}$/InP diode lasers emitting at 1.1 μm, with room-temperature pulsed thresholds as low as 2.8 kA/cm^2, have been fabricated by liquid-phase epitaxy on melt-grown InP substrates.

PACS numbers: 42.60.J, 42.80.S

This letter reports the room-temperature operation of $Ga_{1-x}In_xAs_{1-y}P_y$/InP double-heterostructure (DH) diode lasers. Broad-area devices emitting at 1.1 μm have been fabricated from three-layer films grown by liquid-phase epitaxy (LPE) on InP substrates. Pulsed thresholds as low as 2.8 kA/cm^2 have been obtained for an active region thickness of 0.6 μm. With threshold in this range it should be possible to produce stripe-geometry lasers capable of continuous operation at room temperature. Such cw lasers would be of particular interest for communication systems using optical fibers, which have their minimum transmission loss near 1.1 μm.[1]

Three different active-layer/barrier-layer combinations have been used for DH diode lasers emitting at wavelengths near 1 μm: $Ga_{1-x}In_xAs/Ga_{1-y}In_yP$ (Ref. 2), $GaAs_{1-x}Sb_x/Ga_{1-y}Al_yAs_{1-x}Sb_x$ (Ref. 3), and $Ga_{1-x}In_xAs_{1-y}P_y$/InP (Ref. 4). Pulsed room-temperature operation has been reported for the first[2] and second[3] combinations, in both of which the active layer is a ternary alloy between GaAs and a lower-band-gap III-V compound. Since GaAs differs significantly in lattice constant from both ternaries, in each case the barrier layers must be formed by another alloy, whose composition can be adjusted to give the high degree of active/barrier lattice matching that is essential for efficient laser operation. Consequently, the compositions of three layers—the active region and both barriers—must be accurately controlled for optimum device performance. Furthermore, to obtain epitaxial layers of sufficiently high quality, it is necessary to grow intermediate alloy layers with either continuous or step-wise composition grading on the GaAs substrates before deposition of the heterostructures. In preparing GaAsSb/GaAlAsSb layers, for example, three GaAsSb layers of different compositions have been grown between the substrate and the first GaAlAsSb barrier.[3]

Operation of DH diode lasers utilizing GaInAsP active regions has previously been limited to 77 K, both for emission near 1 μm (Ref. 4) and for emission near 0.6 μm (Ref. 5). However, the quaternary alloy offers several potential advantages because the presence of four components makes it possible to obtain the same lattice constant as that of InP over a range of compositions that give energy gaps corresponding to any wavelength between 0.92 and 1.7 μm.[6] For 1.1 μm or any other wavelength in this range, only the composition of the active region requires accurate control in order to achieve excellent (in principle, perfect) lattice matching to barrier layers of InP, whose composition is fixed because this compound has a narrow homogeneity region. The possibility of such accurate control has been demonstrated by the LPE growth of GaInAsP layers on InP for photoemissive devices[7] as well as for diode lasers.[4] Furthermore, the LPE growth procedure is simplified because the heterostructure layers can be grown directly on InP substrates, without the need for intermediate composition-graded alloy layers. In addition, the elimination of lattice mismatch from the entire device structure should cause a reduction in defects and strain, and therefore might result in longer operating lifetimes.

To prepare lasers that emit at 1.1 μm, successive layers of p-doped InP, undoped $Ga_{0.12}In_{0.88}As_{0.23}P_{0.77}$, and n-doped InP were grown on InP substrates in a horizontal sliding boat machined from high-purity graphite. The substrates were (111)-oriented wafers cut from a Zn-doped ingot ($p = 4\times10^{18}$ cm^{-3}) grown from a stoichiometric melt by the horizontal gradient-freeze technique.[8] The 111-B substrate surface was ground with 2-μm alumina and then chem-mech polished with Br-CH_3OH. All LPE layers were grown at a cooling rate of 0.7 C/min from In-rich solutions that were supercooled by 3–10 C below their saturation temperatures before placing them in contact with the substrate at temperatures near 635 C. As in the case of GaAs and GaAlAs (Ref. 9), the supercooling technique yields smooth flat layers of uniform thickness. The growth solutions for the p- and n-type InP layers were doped with sufficient Zn and Sn, respectively, to give carrier concentrations of about 3×10^{18} cm^{-3} according to published distribution data.[10,11] The p-type InP layers were ~5 μm thick, the n-type InP layers ~2 μm thick, and the GaInAsP layers from 0.2 to 2 μm thick. The active layers were too thin for accurate electron microprobe analysis. The composition of $Ga_{0.12}In_{0.88}As_{0.23}P_{0.77}$ was found by analyzing somewhat thicker layers grown under the same experimental conditions. (Although in principle active layers could be grown directly on the InP substrate, this procedure would yield imperfect layers because some decomposition of the substrate occurs by preferential evaporation of P during the heating period before LPE growth. Better heterostructures are obtained by first depositing an InP layer and then immediately growing the GaInAsP layer before decomposition can occur.)

After being removed from the LPE growth furnace, the wafer was ground on the substrate side to reduce its over-all thickness to about 100 μm. Contacts to the ground p-type surface and to the as-grown n-type sur-

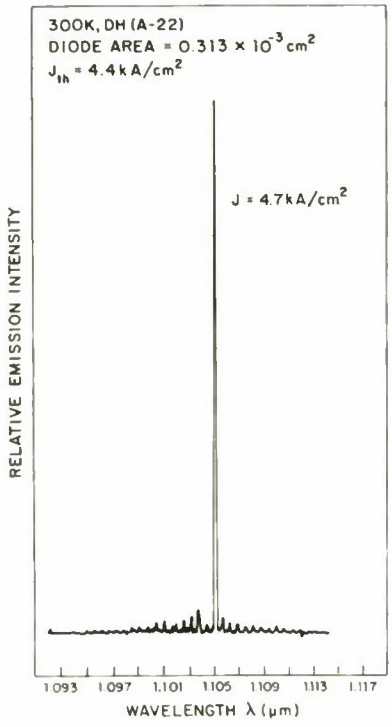

FIG. 1. Room-temperature emission spectrum of pulsed GaInAsP/InP DH laser for drive current density about 10% above threshold.

face were made by evaporating Au/Zn and Au/Sn, respectively, and alloying at 350 °C. The wafer was then sawed and cleaved to form diodes with Fabry-Perot cavities. A preliminary evaluation of the diodes was made by using an infrared microscope to examine their spontaneous emission under forward bias. The radiation observed from properly lattice-matched structures originates mainly from the active region, but the emission is very weak or undetectable from active regions with compositions that do not give the same lattice constant as InP.

Figure 1 is the room-temperature spectrum of a DH diode with an active region about 0.6 μm thick, measured at a current density about 10% above the laser threshold (J_{th}). The radiation is concentrated almost entirely in a single peak at 1.105 μm. From the spacing of the cavity modes, which extend from 1.095 to 1.113 μm, the effective refractive index is found to be about 5.1. The photon energy at the peak is 1.12 eV, about 50 meV less than the energy gap given for $Ga_{0.12}In_{0.88}As_{0.23}P_{0.77}$ by a published empirical relationship.[6] Such differences are generally observed for diode lasers because most of the lasing transitions involve impurity levels.

For an active region thickness (d) of 2 μm, $J_{th} \approx 16$ kA/cm². As d is decreased, the value of J_{th} decreases

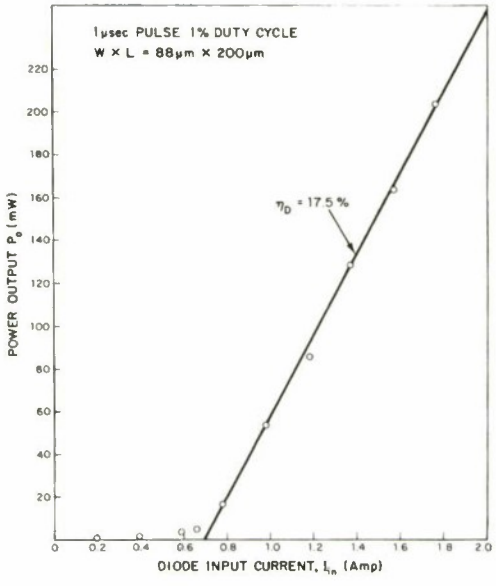

FIG. 2. Room-temperature power output (P_0) of pulsed GaInAsP/InP DH laser vs input current (I_{in}).

linearly with d, reaches a minimum of ~3 kA/cm² at ~0.4 μm, and then increases rapidly. The lowest value of J_{th} so far obtained is 2.8 kA/cm², which was measured for a diode with $d = 0.6$ μm and a cavity length (L) of 475 μm. In the linear region, the J_{th} values are about 70% higher than those reported[12] for GaAs/GaAlAs DH lasers with the same values of d. The value of J_{th} for a given GaInAsP/InP diode decreases by about a factor of 20 from 300 to 77 K.

The variation of the total output power (P_0) emitted from both faces of a typical diode is plotted against input current (I_{in}) in Fig. 2. The diode was driven by 1-μsec pulses with a duty cycle of 1%, and the output was measured with a calibrated Si photodiode. The threshold current is about 0.7 A. Above threshold the differential external quantum efficiency is 17.5%, about one-

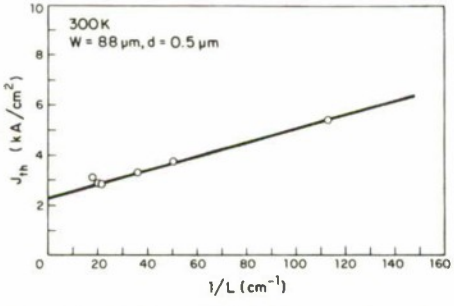

FIG. 3. Threshold current (J_{th}) vs $1/L$, where L is the cavity length, for pulsed GaInAsP/InP DH lasers emitting at 1.1 μm.

third the values for state-of-the-art GaAs/GaAlAs DH lasers,[12] and the differential power efficiency is 9.5%. At $2J_{th}$, the total output power is 135 mW, and the over-all power efficiency is 4.9%.

For lasers with $d = 0.5$ μm and values of L between 90 and 500 μm, J_{th} is found to vary linearly with $1/L$, as shown in Fig. 3. For the relationship $J_{th} = \alpha/\beta + (1/L\beta) \ln (1/R)$, where α is the loss, β is the gain, and $R \approx 0.29$ is the reflectivity of the active layer, the experimental data give $\alpha = 68$ cm^{-1} and $\beta = 30$ cm (kA)$^{-1}$. The differential internal quantum efficiency calculated from α and β is 37%, about half the value for GaAs/GaAlAs DH lasers.[12]

In conclusion, the excellent properties of the DH GaInAsP/InP diode lasers even at this early stage of development, together with their structural simplicity and consequent ease of fabrication, make them promising devices for applications in optical communications and integrated optical circuits.

The author is grateful to A.J. Strauss for encouraging this work, M.C. Finn for performing the electron microprobe analysis, S.R. Chinn for obtaining the room-temperature emission spectra, and J.A. Rossi for measuring the laser output power. He thanks R.E. Nahory for communicating his results prior to publication. The technical assistance of M.J. Button and T.A. Lind is also deeply appreciated.

•Work sponsored by the Department of the Air Force.

[1]L.G. Cohen, P. Kaiser, J.B. MacChesney, P.B. O'Connor, and H.M. Presby, Appl. Phys. Lett. **26**, 472 (1975).
[2]C.J. Nuese and G.H. Olson, Appl. Phys. Lett. **26**, 528 (1975).
[3]K. Sugiyama and H. Saito, Jpn. J. Appl. Phys. **11**, 1057 (1972); R.E. Nahory and M.A. Pollack, Appl. Phys. Lett. **27**, 562 (1975).
[4]A.P. Bogatov, L.M. Dolginov, L.V. Druzhinina, P.G. Eliseev, B.N. Sverdlov, and E.G. Shevchenko, Sov. J. Quantum. Electron. **4**, 1281 (1975).
[5]W.R. Hitchens, N. Holonyak, Jr., P.D. Wright, and J.J. Coleman, Appl. Phys. Lett. **27**, 245 (1975).
[6]R.L. Moon, G.A. Antypas, and L.W. James, J. Electron. Mater. **3**, 635 (1974).
[7]G.A. Antypas and R.L. Moon, J. Electrochem. Soc. **120**, 1574 (1973).
[8]K.J. Bachmann and E. Buehler, J. Electron. Mater. **3**, 279 (1974).
[9]J.J. Hsieh, J. Cryst. Growth **27**, 49 (1974).
[10]M.G. Astles, F.G.H. Smith, and E.W. Williams, J. Electrochem. Soc. **120**, 1751 (1973).
[11]F.G. Rosztoczy, G.A. Antypas, and C.J. Casan, in *Proceedings of the Third International Symposium on GaAs and Related Compounds* (Institute of Physics, London, 1971), p. 86.
[12]See review by M.B. Panish, IEEE Trans. Microwave Theory Tech. **MTT-23**, 20 (1975).

APPENDIX B

[Reprinted with permission
from Appl. Phys. Lett. 28, No. 12,
709-711 (15 June 1976)]

Room-temperature cw operation of GaInAsP/InP double-heterostructure diode lasers emitting at 1.1 μm*

J. J. Hsieh, J. A. Rossi, and J. P. Donnelly

Lincoln Laboratory, Massachusetts Institute of Technology, Lexington, Massachusetts 02173
(Received 1 March 1976)

Room-temperature cw operation has been achieved for stripe-geometry double-heterostructure $Ga_{0.12}In_{0.88}As_{0.23}P_{0.77}$/InP diode lasers emitting at 1.1 μm. The heterostructures were grown by liquid-phase epitaxy on melt-grown InP substrates, and stripes were defined by using proton bombardment to produce high-resistance current-confining regions.

PACS numbers: 42.60.Jf, 42.82.+n, 85.60.Dw

Pulsed operation at liquid-nitrogen temperature[1] and at room temperature[2,3] has been reported for double-heterostructure (DH) diode lasers with a $Ga_xIn_{1-x}As_yP_{1-y}$ active region lattice matched to InP barrier layers. In this letter we report the cw room-temperature operation of GaInAsP/InP DH lasers. The emission of these lasers occurs at ~1.1 μm, a wavelength that is advantageous for fiber optics communication systems because it falls in a spectral region where the transmission losses[4,5] and dispersion[5] of high-quality glass fibers are both low. This is the longest emission wavelength so far reported for diode lasers that operate continuously at room temperature. The only other such devices are the GaAs/GaAlAs[6,7] and GaAsSb/GaAlAsSb[8] DH lasers, for which emission has been obtained from 0.7 to 0.9 μm and at 1.0 μm, respectively.

The GaInAsP/InP heterostructures were grown on (111)-oriented InP substrates by a supercooled liquid-phase epitaxial (LPE) technique.[9] The procedure was similar to the one used in preparing pulsed lasers,[3] but the substrates were n-type wafers ($n \sim 2\times10^{18}$ cm^{-3}) cut from a Sn-doped Czochralski-grown crystal, rather than the p-type Zn-doped wafers used previously. The 111-B substrate surface was ground with 2-μm alumina, chemi-mech polished with Br-CH_3OH, and then free etched with Br-CH_3OH to remove an additional 10 μm. Three layers were grown sequentially on the substrate: an n-type InP layer (Sn-doped, $n \sim 4\times10^{18}$ cm^{-3}), an n-type $Ga_{0.12}In_{0.88}As_{0.23}P_{0.77}$ active region (either undoped or Sn-doped,[10] $n \sim 1-3\times10^{17}$ cm^{-3}), and a p-type InP barrier layer (Zn-doped, $p \sim 3\times10^{18}$ cm^{-3}). Figure 1 is an optical micrograph of the cleaved edge of a heterostructure that had been etched in a solution of $K_3Fe(CN)_6$ and KOH. The active layer is ~0.5 μm thick, and the InP barrier layers are each ~2 μm thick.

Stripe-geometry lasers were fabricated by a proton bombardment technique[11] similar to the one used in preparing GaAs/GaAlAs lasers of this type.[12] The as-grown surface of the upper InP layer was plated with 25-μm-wide Au stripes on 250-μm centers, after which this surface was bombarded with a 2×10^{15} cm^{-2} dose of 180-keV protons. While the areas beneath the Au stripes were shielded from the protons and therefore unaffected by the bombardment, the unprotected areas were rendered highly resistive to a depth ~1.8 μm, approximately the thickness of the top InP layer. As a result of this treatment, during diode operation the current was confined to the narrow regions that had remained low in resistance.

After bombardment, the Au stripes were etched off, and the wafer was lapped on the substrate side to a thickness of ~100 μm. Contacts were made by evaporating Au/Zn (~10 wt% Zn) and Au/Sn (~20 wt% Sn) onto the p and n-type sides, respectively, and alloying by means of a 10-sec 420 °C drive-in cycle. The wafer was then cleaved into bars and sawed between adjacent stripes to obtain individual diodes. A number of diodes found to have pulsed laser thresholds of 6 kA/cm^2 or less were tested for cw operation. Each of these devices was mounted, p side down, on a type-IIA diamond heatsink that was mounted on a Cu stud embedded in a large Cu block, through which methanol flowed continuously to help maintain temperature stability.

To measure the cw diode output, the light emitted from one face was chopped at 80 Hz and detected by a Si solar cell (with a calibrated sensitivity of 0.04 mA/mW) in series with a 10-Ω load. The voltage across the load was amplified and displayed on an oscilloscope. The measured output of a typical diode is plotted against input current in Fig. 2. The laser threshold is seen to be ~330 mA ($J_{th} \sim 7.5$ kA/cm^2). At a current of 425 mA the output power radiated from one face is ~6 mW, and the corresponding differential efficiency (η_D) is ~10%. The lowest cw threshold we have so far obtained is 265 mA ($J_{th} \sim 4.7$ kA/cm^2).

For pulsed operation of the diode of Fig. 2 at a very low duty cycle (100-nsec pulses, 75 pps) the values of

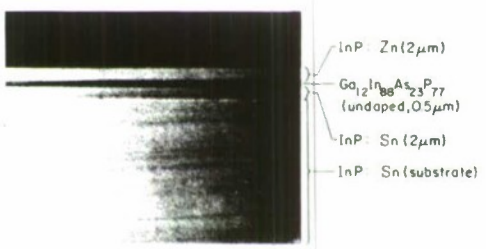

FIG. 1. Cleaved edge of GaInAsP/InP double heterostructure.

J_{th} and η_D are 4.3 kA/cm^2 and 20%, respectively. The increase in threshold and decrease in efficiency with increasing duty cycle, which are characteristic of semiconductor lasers, are attributable to heating. We expect to achieve a significant reduction in heating by using improved contacting techniques to reduce the diode series resistance (which is 3 Ω for the laser of Fig. 2) and to improve the heat dissipation.

For broad-area diodes of the same length and made from the same wafer as the diode of Fig. 2, the pulsed threshold is ~4.9 kA/cm^2. The close agreement between the pulsed thresholds for the broad-area and stripe-geometry devices indicates that losses due to incomplete lateral current confinement are small for the 25-μm stripe laser. The minimum stripe width that permits effective current confinement is primarily determined by the diffusion length of injected carriers,[13] which had not been accurately determined for the GaInAsP composition used here.

Figure 3 shows the cw emission spectrum obtained for another stripe-geometry diode just above threshold. The diode radiation was dispersed by a 1-m spectrometer and detected with a cooled S-1 photomultiplier. A broad emission band of ~250 Å like the one shown in Fig. 3 was observed for a number of the cw lasers, although others had bandwidths as narrow as 150 Å. We do not know the origin of the broad emission, which is also observed for some heavily Si-doped GaAs lasers,[14] or the reason for the bandwidth variation from diode to diode. From the mode spacing of ~6.6 Å in Fig. 3, together with the diode length of ~230 μm, the effective index of refraction (including dispersion effects) is calculated to be ~4.1, a typical value for III-V compounds.

Now that their cw operation at room temperature has been demonstrated, the GaInAsP/InP DH lasers should be seriously considered as radiation sources for communication systems using fiber optics. These lasers (like the GaInAsP DH lasers[15] that emit near 0.6 μm) have the advantage that the active region has the same lattice constant as the substrate used for LPE growth.

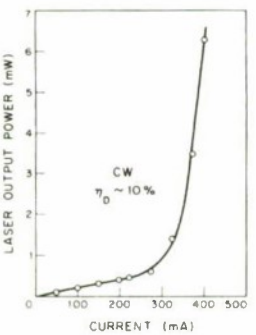

FIG. 2. Power emitted from one face of a cw GaInAsP/InP double-heterostructure diode laser as a function of input current.

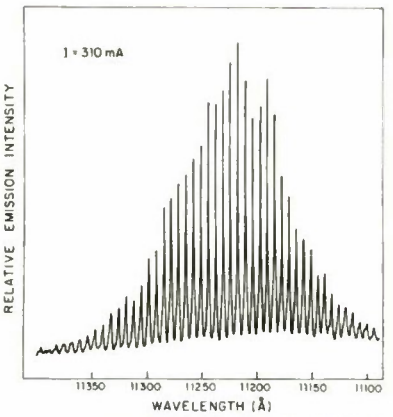

FIG. 3. Emission spectrum for GaInAsP/InP diode laser operated just above threshold.

This makes preparation considerably simpler than in the case of the GaAsSb/GaAlAsSb[8] and GaInAs/GaInP[16] DH lasers emitting near 1.0 μm, both of which require the growth of intermediate composition-graded alloy layers in order to adjust the lattice mismatch between the substrate and the active region. Since lattice matching to InP is possible for GaInAsP alloys with energy gaps as low as 0.7 eV, there should be no difficulty in achieving laser emission at wavelengths well beyond 1.1 μm. In particular, it should be possible to fabricate lasers emitting at 1.25 μm, the wavelength at which some glass fibers are reported to exhibit minimum dispersion.[5] It would not be surprising for such lasers to have still lower thresholds than those reported here, because both the barrier height for current confinement and the refractive index discontinuity for optical guiding will increase as the alloy energy gap decreases.

We thank A.J. Strauss, A.G. Foyt, and I. Melngailis for helpful discussions and M.J. Button, T.A. Lind, and R. Brooks for technical assistance during this work.

*Work sponsored by the Department of the Air Force.

[1]A.P. Bogatov, L.M. Dolginov, L.V. Druzhinina, P.G. Eliseev, B.N. Sverdlov, and E.G. Shevchenko, Sov. J. Quantum Electron. **4**, 1281 (1975).
[2]A.P. Bogatov, L.M. Dolginov, P.G. Eliseev, M.G. Mil'vidsky, B.N. Sverdlov, and E.G. Shevchenko, Fiz. Tekh. Tekh. Poluprov. **9**, 1956 (1975).
[3]J.J. Hsieh, Appl. Phys. Lett. **28**, 283 (1976).
[4]L.G. Cohen, P. Kaiser, J.B. MacChesney, P.B. O'Connor, and H.M. Presby, Appl. Phys. Lett. **26**, 472 (1975).
[5]D.N. Payne and W.A. Gambling, Electron. Lett. **11**, 176 (1975).
[6]I. Hayashi, M.B. Panish, P.W. Foy, and S. Sumski, Appl. Phys. Lett. **17**, 109 (1970); Zh.I. Alferov, V.M. Andreev, D.Z. Garbuzov, Y.V. Zhilyaev, E.P. Morozov, E.L. Portnoi, and V.G. Trofim, Sov. Phys.-Semicond. **4**, 1573 (1971).
[7]B.I. Miller, J.E. Ripper, J.C. Dyment, E. Pinkas, and M.B. Panish, Appl. Phys. Lett. **18**, 403 (1971). The emission from these devices was shifted to shorter wavelengths by using GaAlAs alloys for the active region.

[8]R. E. Nahory, M. A. Pollack, E. D. Beebe, J. C. DeWinter, and R. W. Dixon, Appl. Phys. Lett. **28**, 19 (1976).
[9]J. J. Hsieh, J. Cryst. Growth **27**, 49 (1974).
[10]G. M. Blom and J. M. Woodall, Appl. Phys. Lett. **17**, 373 (1970).
[11]A. G. Foyt, W. T. Lindley, C. M. Wolfe, and J. P. Donnelly, Solid-State Electron. **12**, 209 (1969).
[12]J. C. Dyment, L. A. D'Asaro, J. C. North, B. I. Miller, and J. E. Ripper, Proc. IEEE **60**, 726 (1972).
[13]B. W. Hakki, J. Appl. Phys. **44**, 5021 (1973).
[14]J. A. Rossi and J. J. Hsieh, Appl. Phys. Lett. **21**, 287 (1972).
[15]W. R. Hitchens, N. Holonyak, Jr., P. D. Wright, and J. J. Coleman, Appl. Phys. Lett. **27**, 245 (1975).
[16]C. J. Nuese and G. M. Olson, Appl. Phys. Lett. **26**, 528 (1975).

UNCLASSIFIED

SECURITY CLASSIFICATION OF THIS PAGE *(When Data Entered)*

REPORT DOCUMENTATION PAGE		READ INSTRUCTIONS BEFORE COMPLETING FORM
1. REPORT NUMBER ESD-TR-77-171	2. GOVT ACCESSION NO.	3. RECIPIENT'S CATALOG NUMBER
4. TITLE *(and Subtitle)* Electrooptical Devices		5. TYPE OF REPORT & PERIOD COVERED Semiannual Technical Summary 1 October 1976 – 31 March 1977
		6. PERFORMING ORG. REPORT NUMBER
7. AUTHOR*(s)* Ivars Melngailis and Arthur G. Foyt, Jr.		8. CONTRACT OR GRANT NUMBER*(s)* F19628-76-C-0002
9. PERFORMING ORGANIZATION NAME AND ADDRESS Lincoln Laboratory, M.I.T. P.O. Box 73 Lexington, MA 02173		10. PROGRAM ELEMENT, PROJECT, TASK AREA & WORK UNIT NUMBERS Program Element Nos. 62702F and 61102F Project No. 261104
11. CONTROLLING OFFICE NAME AND ADDRESS Rome Air Development Center Griffiss AFB, NY 13440		12. REPORT DATE 31 March 1977
		13. NUMBER OF PAGES 36
14. MONITORING AGENCY NAME & ADDRESS *(if different from Controlling Office)* Electronic Systems Division Hanscom AFB Bedford, MA 01731		15. SECURITY CLASS. *(of this report)* Unclassified
		15a. DECLASSIFICATION DOWNGRADING SCHEDULE

16. DISTRIBUTION STATEMENT *(of this Report)*

Approved for public release; distribution unlimited.

17. DISTRIBUTION STATEMENT *(of the abstract entered in Block 20, if different from Report)*

18. SUPPLEMENTARY NOTES

None

19. KEY WORDS *(Continue on reverse side if necessary and identify by block number)*

electrooptical devices	proton bombardment	ion implantation
avalanche photodiodes	double-heterostructure	GaInAsP/InP lasers

20. ABSTRACT *(Continue on reverse side if necessary and identify by block number)*

The current objectives of the electrooptical device program are: (1) to perform life tests on GaInAsP/InP double-heterostructure (DH) diode lasers operating in the 1.0- to 1.2-μm wavelength region and analyze the degradation mechanisms, and (2) to fabricate and study avalanche photodiodes of similar composition GaInAsP operating in the same wavelength region.

In the diode laser part of the program, 11 DH GaInAsP/InP lasers, operating continuously at room temperature, have been placed on life test. The first three devices, fabricated from one wafer, have logged over 4000, 3600, and 3200 hours, respectively, without degradation, and are still in operation. The eight devices fabricated from two additional wafers also show no evidence

DD FORM 1 JAN 73 1473 EDITION OF 1 NOV 65 IS OBSOLETE

UNCLASSIFIED

SECURITY CLASSIFICATION OF THIS PAGE *(When Data Entered)*

20. ABSTRACT *(Continued)*

of internal degradation. However, a laser end-face contamination problem is present in several of the newer devices. Although this contamination can be removed from most of the devices by simple cleaning, improved fabrication procedures are currently being developed to eliminate the sources of the contamination.

The p-n junction location in DH GaInAsP/InP diode lasers has been determined by use of a scanning electron microscope. Even though undoped or Sn-doped quaternary layers are n-type if grown on insulating substrates, the quaternary layers in the lasers are p-type, presumably due to Zn diffusion from the Zn-doped InP capping layer.

As part of the avalanche photodiode program, proton bombardment and ion implantation in InP have been investigated for use in diode fabrication. A study of proton bombardment in InP indicates that the resistivity of n-type InP can be increased only to a level of about 10^3 Ω-cm, while the resistivity of p-type InP can be increased to $>10^8$ Ω-cm for an optimum multiple-energy dose or an optimum combination of dose and post-bombardment anneal. The results can be explained by a model which assumes that the proton bombardment creates both deep donor and deep acceptor levels.

The ion implantation of Se, Si, Be, Mg, Cd, and Fe in InP is under investigation. As expected, Se and Si implants followed by a 750°C, 15-min. anneal result in n-type layers, while Be, Mg, and Cd implants followed by a similar anneal result in p-type layers. Implantation of Fe has been found to be quite effective in creating high-resistivity layers in n-type InP. A multi-energy Fe implant in n-type InP ($n \approx 4 \times 10^{16}$ cm^{-3}) followed by annealing at 725°C for 15 min. yields layers with a resistivity of approximately 10^7 Ω-cm.

In the liquid-phase epitaxy (LPE) of InP for avalanche photodiodes, a high distribution coefficient impurity, identified as silicon, has been shown to be a key problem in achieving required high-purity layers. It was found not only that the Si concentration of as-received In is too high, but also that the LPE growth solution can be contaminated with Si through direct or indirect contact with quartz if a strongly reducing gas such as dry H_2 is present in the growth tube.